Chemical Isolation in the Asian monsoon anticyclone observed in Atmospheric Chemistry Experiment (ACE-FTS) data

M. Park, W. J. Randel, L. K. Emmons, P. F. Bernath, K. A. Walker, C. D. Boone

Atmos. Chem. Phys. Discuss., 7, 13839–13860, 2007
www.atmos-chem-phys-discuss.net/7/13839/2007/

Atmospheric Chemistry and Physics Discussions

Chemical isolation in the Asian monsoon anticyclone observed in Atmospheric Chemistry Experiment (ACE-FTS) data

M. Park[1], W. J. Randel[1], L. K. Emmons[1], P. F. Bernath[2,3], K. A. Walker[2,*], and C. D. Boone[2]

[1]National Center for Atmospheric Research, Boulder, Colorado, USA
[2]Department of Chemistry, University of Waterloo, Waterloo, Ontario, Canada
[3]Department of Chemistry, University of York, Heslington, York, UK
[*]now at: Department of Physics, University of Toronto, Toronto, Ontario, Canada

Received: 2 August 2007 – Accepted: 13 September 2007 – Published: 25 September 2007

Correspondence to: M. Park (mijeong@ucar.edu)

Abstract

Evidence of chemical isolation in the Asian monsoon anticyclone is presented using chemical constituents obtained from the Atmospheric Chemistry Experiment Fourier Transform Spectrometer instrument during summer (June–August) of 2004–2006. Carbon monoxide (CO) shows a broad maximum over the monsoon anticyclone region in the upper troposphere and lower stratosphere (UTLS); these enhanced CO values are associated with air pollution transported upward by convection, and confined by the strong anticyclonic circulation. Profiles inside the anticyclone show enhancement of tropospheric tracers CO, HCN, C_2H_6, and C_2H_2 between ~12 to 20 km, with maxima near 13–15 km. Strong correlations are observed among constituents, consistent with sources from near-surface pollution and biomass burning. Stratospheric tracers (O_3, HNO_3 and HCl) exhibit decreased values inside the anticyclone between ~12–20 km. These observations are further evidence of transport of lower tropospheric air into the UTLS region, and isolation of air within the anticyclone. The relative enhancements of tropospheric species inside the anticyclone are closely related to the photochemical lifetime of the species, with strongest enhancement for shorter lived species. Vertical profiles of the ratio of C_2H_2/CO (used to measure the relative age of air) suggest relatively rapid transport of fresh emissions up to tropopause level inside the anticyclone.

1 Introduction

The Asian summer monsoon is the dominant circulation feature spanning Southeast Asia to Afghanistan during Northern Hemisphere (NH) summer. The Asian monsoon circulation is a thermally direct circulation dominated by a low-level thermal low and an upper-level anticyclone (Krishnamurti and Bhalme, 1976). Flanked by the equatorial and subtropical jets, the anticyclone acts as strong transport barrier to chemical constituents, such as water vapor (Dethof et al., 1999) and ozone (Randel and Park, 2006), in the upper troposphere and lower stratosphere (UTLS). Carbon monoxide

ACPD

7, 13839–13860, 2007

transported upwards by the monsoon convection is trapped within the monsoon anticyclone in the upper troposphere (Li et al., 2005). Recent satellite observations have highlighted the strong isolation of carbon monoxide within the monsoon anticyclone, extending into the lower stratosphere (Fu et al., 2006; Park et al., 2007).

The Atmospheric Chemistry Experiment (ACE) is a Canadian-led satellite mission launched in 2003. The ACE Fourier Transform Spectrometer (ACE-FTS) instrument provides vertical profiles of a few dozen chemical species covering the middle troposphere to thermosphere (~10–100 km), with data available from the polar regions to the tropics (Bernath et al., 2005). In this study we use ACE-FTS measurements to explore the consequences of vertical transport within the Asian monsoon anticyclone. In particular, we focus on the ACE-FTS measurements of carbon monoxide (CO), hydrogen cyanide (HCN), ethane (C_2H_6) and acetylene (C_2H_2), which have common sources of biomass burning (Andreae and Merlet, 2001) and major sinks of reaction with hydroxyl radical (Logan et al., 1981). The photochemical lifetimes of these species span the range of 0.5–5 months, which make them useful as tracers of transport in the troposphere and lower stratosphere. We also include analyses of CH_3Cl, which is produced by biomass burning and has a lifetime of about a year (Blake et al., 1996; Yoshida et al., 2004), and OCS, with sources of anthropogenic and oceanic emissions (Watts, 2000) and a lifetime of several years (Chin and Davis, 1995; Blake et al., 2004).

Numerous observational studies of tropospheric pollutants have been made based on aircraft observations (e.g., Smyth et al., 1996; Blake et al., 1996; Talbot et al., 1999; Singh et al., 2003; Russo et al., 2003). However, space-based observations are limited and relatively new. Tropospheric CO has been obtained from several satellite instruments, including Measurement of Air Pollution from Satellites (Connors et al., 1999), Interferometric Monitor for Greenhouse gases (Clerbaux et al., 2003), Measurements Of Pollution In The Troposphere (Deeter et al., 2004; Edwards et al., 2006), Microwave Limb Sounder (Waters et al., 2006), and Tropospheric Emission Spectrometer (Beer, 2006), and these data have been used for studies of tropospheric pollution and long-range transport. However, ACE–FTS has the advantage of simultaneous retrieval of

ACPD
7, 13839–13860, 2007

numerous species in addition to CO. A few previous studies have used ACE-FTS measurements of CO, HCN, C_2H_6, C_2H_2 and methanol (CH_3OH) to study the effect of biomass burning emissions in the UTLS region (Rinsland et al., 2005; Dufour et al., 2006; Coheur et al., 2007), and our work extends those analyses with focus on the Asian monsoon region.

2 Data description

The ACE mission was launched on 12 August 2003 into a high inclination (74°) circular orbit at 650 km altitude. The high resolution infrared ACE-FTS measures solar absorption spectra from 750 to 4400 cm^{-1} using the solar occultation technique. The primary goal of the ACE mission is focused on polar ozone chemistry and dynamics, and the majority of measurements are obtained over high latitudes (Bernath et al., 2005). The vertical field of view of the instrument is 3 km, and measurements during each occultation are obtained with a vertical sampling of 2–6 km (depending on the angle of the sun with respect to the spacecraft velocity vector); the constituent profile retrievals are available on an (oversampled) 1 km vertical grid (Boone et al., 2005). The data here are based on version 2.2 retrievals (including the ozone update). The C_2H_6 and C_2H_2 data are research products retrieved to higher altitudes for this study, and we focus on observations during NH summer (June–August) of 2004–2006. Due to the orbit geometry, most of the low latitude observations occur in August during this period.

The chemical species analyzed here include tropospheric constituents CO, HCN, C_2H_6, C_2H_2, OCS, and CH_3Cl, and stratospheric species O_3, HNO_3, and HCl. The photochemical lifetimes of these constituents, which span the range from ~1 month to longer than 1 year, are provided in Table 1. These numbers are estimated in the troposphere but are almost constant up to the UTLS region. For data screening purposes, we exclude profiles with values outside of three-sigma variance between 60° S and 60° N. This method typically excludes less than 1% of profiles depends on the species. The initial comparisons of version 1.0 ACE-FTS retrievals show fairly good agreement

ACPD
7, 13839–13860, 2007

between 15 and 40 km for ozone (Walker et al., 2005) and 20–100 km for CO (Jin et al. 2005). Papers detailing the validation studies for version 2.2 products (including the ozone "update") are in preparation (for ozone: Dupuy et al., 2007[1]; for CO: Clerbaux et al., 2007[2]). The estimated fitting error of version 2.2 CO and version 2.2 ozone update are 2–6% and 2–7% in the UTLS region, respectively.

3 Chemical isolation in the anticyclone

Figure 1a shows CO mixing ratio amounts at 16.5 km for all of the ACE-FTS observations during June–August 2004–2006. The majority of points at mid to high latitudes lie in the stratosphere (where CO≤20 parts per billion by volume, ppbv) and in the upper troposphere (where CO ranges 40–50 ppbv, see Clerbaux et al., 2005). There is a broad maximum in CO over the Asian monsoon region (0°–120° E and 10°–40° N), and a similar maximum is evident for altitudes ~12–20 km (not shown). HCN mixing ratios (Fig. 1b) also exhibit a maximum in this region, roughly coincident with the CO maximum. Daily observations of CO from MLS data have demonstrated that CO maxima at 100 hPa (~16 km) occur within the Asian monsoon anticyclone throughout summer (Park et al., 2007), and the highest CO values seen in Fig. 1a likely represent individual ACE-FTS measurements within the anticyclone. To examine the behavior of other atmospheric constituents in the monsoon anticyclone, we use the CO values to identify profiles within the boundary of the anticyclone (i.e., the high values in Fig. 1a). Profiles 'inside' are defined where CO is higher than 60 ppbv at 16.5 km (see Fig. 1a) and the rest of the profiles between 10°–40° N are regarded as "outside" the anticyclone (representing background conditions). Based on this definition, there are ~40

[1] Dupuy, E., Walker, K. A., Kar, J., et al.: Validation of ozone measurements from the Atmospheric Chemistry Experiment (ACE), to be submitted, Atmos. Chem. Phys., 2007.

[2] Clerbaux, C., George, M., Walker, K. A., et al.: CO measurements from the ACE-FTS satellite instrument: data analysis and validation using ground-based, airborne and spaceborne observations, submitted, Atmos. Chem. Phys. Discuss., 2007.

profiles inside and ~240 profiles outside the anticyclone at 16.5 km for observations over June–August 2004–2006.

We compare in Fig. 2 the average vertical profiles of tropospheric constituents (CO, HCN, C_2H_6, C_2H_2, CH_3Cl and OCS) inside and outside of the anticyclone, respectively. For each group of profiles we calculate the mean and the standard error of the mean (the sample standard deviation, divided by the square root of the number of observations, shown as error bars in Fig. 2). Substantial enhancements within the anticyclone are observed for CO, HCN, C_2H_6, and C_2H_2 in Fig. 2, with significant differences up to ~20 km. While the outside or background profiles exhibit monotonic decreases with altitude, profiles inside the anticyclone show significant maxima near 15 km for CO, HCN and C_2H_6, and near 13 km for C_2H_2 (which has a significantly shorter lifetime, Table 1). The long-lived tracers (CH_3Cl and OCS) show slight enhancements within the anticyclone over ~14–18 km (Figs. 2e and f). The higher mixing ratios within the anticyclone probably result from a combination of rapid vertical transport and horizontal confinement (Li et al., 2005; Randel and Park, 2006), and the elevated mixing ratios can be regarded as 'fingerprints' of the near-surface pollutant concentrations. In contrast, the outside or background profiles represent photochemically aged air, so that the inside-outside differences may be dependent on the lifetime of the individual species (as explored below). We note that the average mixing ratios shown in Fig. 2 are within the range of those obtained in aircraft field measurements in the lower and middle troposphere (Smyth et al., 1999; Blake et al., 1999; Singh et al., 2003; Xiao et al., 2007).

Figure 3 compares inside versus outside profiles for the stratospheric tracers - O_3, HNO_3 and HCl. Each of these tracers shows reduced mixing ratios inside the anticyclone over ~12–20 km compared to outside profiles, and this behavior is consistent with enhanced transport of tropospheric air into the anticyclone. These observations are consistent with the relative minimum in ozone within the anticyclone shown in Randel and Park (2006) and Park et al. (2007).

Tracer-tracer correlations are useful to diagnose air mass characteristics and rela-

ACPD
7, 13839–13860, 2007

tionships among different species. Figure 4 shows scatter plots of tropospheric tracers versus CO, for HCN, C_2H_6, C_2H_2, OCS and CH_3Cl (for data at 16.5 km). Overall, each of the tropospheric tracers show strong correlations with CO, with high CO values inside the anticyclone (orange plus signs) associated with high values of other species. C_2H_6 and C_2H_2 exhibit relatively compact correlations with CO, suggesting similar sources for these species (Blake et al., 2003). There is significantly more scatter in the HCN versus CO diagram than other species (Fig. 4a), which is similar to results from the TRACE-P aircraft observations (figures are not shown, for details of the TRACE-P mission, see Jacob et al., 2003), and this may be a signature of different sources and sinks for HCN and CO (Singh et al., 2003). CH_3Cl and OCS also exhibit some correlation with CO, but relatively smaller differences between inside and outside profiles. Figure 4f shows a scatter plot for two stratospheric tracers (HCl vs. O_3), showing a highly compact relationship. Low ozone inside the anticyclone is also correlated with high CO. The compact relationships between ozone and the other stratospheric tracers (e.g., HF and HNO_3) are consistently found between 15 and 18 km.

If photochemical loss is a primary destruction mechanism for the tropospheric tracers, then the slope of the scatter plots in Fig. 4 should be related to the respective photochemical ages of the species. We test this in a simple way, by including a line in the scatter plots associated with the respective e-folding time of the two species. For example, the line in the C_2H_2 vs. CO diagram has a slope of (CO lifetime / C_2H_2lifetime), or (2 months/0.5 months). These slopes are included for each of the tropospheric tracers in Fig. 4. Overall there is quite reasonable agreement with the observed distributions, which is also almost overlapped with the linear regression fit (not included). For OCS, the correlations are offset toward higher concentration due to its long lifetime. This quantitative agreement is consistent with the differences between air inside and outside the anticyclone being primarily a result of relatively young air inside versus photochemically aged air outside. The agreement in slopes is also consistent with the approximate lifetimes of the constituents as listed in Table 1.

In order to study the vertical profiles of tracers inside the anticyclone in more detail,

ACPD
7, 13839–13860, 2007

we calculate the difference between the mean profiles in Fig. 2, and then normalize the differences for each tropospheric constituent to a maximum value of 1.0 (Fig. 5a). Here we focus on the species CO, HCN, C_2H_6 and C_2H_2, which show the largest enhancements in Fig. 2. The tracer differences in Fig. 5a have maxima near 15 km, where the monsoon anticyclonic circulation is strong (Randel and Park, 2006). The exact altitudes of maximum values differ somewhat among the tracers (~15 km for CO and HCN, ~17 for C_2H_6 and ~13 km for C_2H_2), but these differences are not emphasized given the 3 km field of view of the ACE-FTS observations. We also include in Fig. 5b the ratio of C_2H_2/CO for the inside and outside profiles, as an indicator of the relative age of an air mass (Smyth et al., 1999; Xiao et al., 2007). The typical range of the ratio is 0.2–2.2 (pptv/ppbv), consistent with the data in Fig. 5b, and a ratio less than one indicates photochemically aged and well-mixed air (Talbot et al., 1999). The C_2H_2/CO ratio inside the anticyclone in Fig. 5b is larger than one, indicating relatively young air transported up to ~16 km. The ratio is less than one outside the anticyclone, signifying photochemically aged and well-mixed air mass as the background.

The level of enhancement inside the anticyclone with respect to the background can be defined as Δ [X]/$[X]_{outside}$*100, where [X] represent the constituent mixing ratio and Δ [X] is $[X]_{inside}$-$[X]_{outside}$ (see Coheur et al., 2007). The enhancement of tropospheric tracers inside the anticyclone is compared in Fig. 6 for different altitudes, plotted as a function of lifetime of the respective species. The enhancement is larger for the shorter-lived constituents and also systematically increases with altitude for C_2H_2, C_2H_6 and CO. The C_2H_2 level increases up to 190 % in Fig. 6 and it can be as large as 2200% for a young biomass burning plume (Coheur et al., 2007). The overall increased enhancement for shorter lifetimes is consistent with relatively young air inside the anticyclone, and older air in the background (as implied for the distributions seen in Fig. 4). There is also a systematic increase in enhancement with altitude over 12–17 km for the shorter-lived species; this may be a signature of systematically older air with higher altitude for the outside or background profiles.

Figure 7 shows the level of enhancement for the stratospheric tracers. Here the val-

ACPD
7, 13839–13860, 2007

ues are negative because these tracers are depleted within the anticyclone as shown in Figs. 3 and 4. There are systematic decreases in the stratospheric tracers over ~11-20 km, with O_3 and HNO_3 decreases up to ~40 % and HCl decreases near ~60%. The vertical profiles of these changes are consistent with the tropospheric tracer enhancement seen in Figure 5a, and the stratospheric tracers provide further evidence of transport of lower tropospheric air to altitudes near and above the tropopause.

4 Summary and discussion

The Asian summer monsoon circulation acts as a transport barrier to the chemical species from upper troposphere to lower stratosphere during NH summer (Li et al., 2005; Randel and Park, 2006; Park et al., 2007). Due to vertical transport from deep convection and strong isolation within the anticyclone, chemical constituents often show relative maxima or minima over the monsoon region. In this study, we show further evidence of chemical isolation in the anticyclone using chemical constituents observed by the ACE-FTS for the period covering summer (June–August) of 2004–2006. ACE-FTS data allow study of constituents with a variety of photochemical lifetimes, and provide information on the detailed vertical structure within the anticyclone.

CO vertical profiles show enhanced values over the monsoon anticyclone from ~12–20 km altitude. The HCN profiles show maxima almost in the same region as CO. Using the clear signal of high CO (Fig. 1a), we define profiles to be "inside" the anticyclone where CO is higher than the threshold (60 ppbv at 16.5 km) and term 'outside' the anticyclone to be the rest of the observations over the latitude band 10°–40° N. The selection of 'inside' profiles is not too sensitive to the threshold values. Averaged profiles inside the anticyclone show strong enhancements for the tropospheric tracers CO, HCN, C_2H_6 and C_2H_2 over approximately 10–20km (Figs. 2 and 5), with relative maxima near 15 km (somewhat lower for C_2H_2). Relatively weak enhancements inside the anticyclone near 15 km are also observed for CH_3Cl and OCS. There are corresponding decreases in stratospheric tracers (O_3, HNO_3 and HCl) inside the anticyclone over the

ACPD
7, 13839–13860, 2007

same altitude range (Figs. 3 and 7). The maxima (minima) in the tropospheric (stratospheric) constituents over 13–15 km may suggest that this is the altitude of strongest outflow from deep convection in the monsoon region. However, this altitude is somewhat higher than the maximum outflow level (~12 km) inferred from tropical radiative balance (Folkins and Martin, 2005) or cloud height estimates (Gettelman et al., 2002; Liu and Zipser, 2005). The distribution of outflow from deep convection in the monsoon region remains an open research topic.

There exist substantial correlations between CO and the tropospheric tracers in the UTLS region. Compact correlations are found between CO and C_2H_6, and between CO and C_2H_2, suggesting common sources for these species. Somewhat higher scatter is observed between CO and HCN, consistent with aircraft observations, and this may signify different sources for the two species. The observed slopes of the correlations among different tropospheric species are in excellent agreement with calculations based on published lifetimes (Fig. 4), and this demonstrates that the differences between profiles inside and outside of the anticyclone are consistent with distinct photochemical ages. This conclusion is consistent with the ratio of (C_2H_2/CO) in Fig. 5b, which suggests relatively younger air inside the anticyclone.

The relative enhancements of tropospheric species inside the anticyclone are closely related to the photochemical lifetime of the species (Fig. 6). The largest enhancements are observed for species with the shortest lifetimes (namely C_2H_2), with relatively small differences found for lifetimes of 1 year or longer. The enhancements are also larger for higher altitudes (between 12 and 17 km), and this may reflect the increase in photochemical age with altitude of species in the background atmosphere. Stratospheric tracers show a ~40–60% decrease within the anticyclone over ~11–20 km altitude range.

Acknowledgements. This work was partially supported under the NASA ACMAP and EOS programs. We thank C. Clerbaux and K. Bowman for discussions and comments on the manuscript. Funding for ACE is provided primarily by the Canadian Space Agency. The National Center for Atmospheric Research is operated by the University Corporation for Atmo-

spheric Research, under sponsorship of the National Science Foundation.

References

Andreae, M. O. and Merlet, P.: Emission of trace gases and aerosols from biomass burning, Global Biogeochem. Cy., 15, 955–966, 2001.

Beer, R.: TES on the Aura Mission: Scientific Objectives, Measurements, and Analysis Overview, IEEE Trans, Geosci. Remote Sensing, 44, 1102–1105, 2006.

Bernath, P. F., McElroy, C. T., Abrams, M. C., et al.: Atmospheric Chemistry Experiment (ACE): Mission overview, Geophys. Res. Lett., 32, L15S01, doi:10.1029/2005GL022386, 2005.

Blake, N. J., Blake, D. R., Sive, B. C., et al.: Biomass burning emissions and vertical distribution of atmospheric methyl halides and other reduced carbon gases in the South Atlantic region, J. Geophys. Res., 101, 24 151–24 164, 1996.

Blake, N. J., Blake, D. R., Wingenter, O. W., et al.: Influence of southern hemispheric biomass burning on midtropopsheric distributions of nonmethane hydrocarbons and selected halocarbons over the remote South Pacific, J. Geophys. Res., 104, 16 213–16 232, 1999.

Blake, N. J., Blake, D. R., Simpson, I. J., et al.: NMHCs and halocarbons in Asian continental outflow during the Transport and Chemical Evolution over the Pacific (TRACE-P) Field Campaign: Comparison With PEM-West B, J. Geophys. Res., 108(D20), 8806, doi:10.1029/2002JD003367, 2003.

Blake, N. J., Streets, D. G., Woo, J.-H., et al.: Carbonyl sulfide and carbon disulfide: Large-scale distributions over the western Pacific and emissions from Asia during TRACE-P, J. Geophys. Res., 109, D15S05, doi:10.1029/2003JD004259, 2004.

Boone, C. D., Nassar, R., Walker, K. A., Rochon, Y., McLeod, S. D., Rinsland, C. P., and Bernath, P. F.: Retrievals for the Atmospheric Chemistry Experiment Fourier Transform Spectrometer, Appl. Opt. 44, 7218–7231, 2005.

Chin, M. and Davis, D. D.: A reanalysis of carbonyl sulfide as a source of stratospheric background sulfur aerosol, J. Geophys. Res., 100(D5), 8993–9006, 10.1029/95JD00275, 1995.

Clerbaux, C., Hadji-Lazaro, J., Turquety, S., Mégie, G., and Coheur, P.-F.: Trace gas measurements from infrared satellite for chemistry and climate applications, Atmos. Chem. Phys., 3, 1495–1508, 2003, http://www.atmos-chem-phys.net/3/1495/2003/.

Clerbaux, C., Coheur, P.-F., Hurtmans, D., Barret, B., Carleer, M., Colin, R., Seme-

niuk, K., McConnell, J. C., Boone, C., and Bernath, P.: Carbon monoxide distribution from the ACE-FTS solar occultation measurements, Geophys. Res. Lett., 32, L16S01, doi:10.1029/2005GL022394, 2005.

Coheur, P.-F., Herbin, H., Clerbaux, C., Hurtmans, D., Wespes, C., Carleer, M., Turquety, S., Rinsland, C. P., Remedios, J., Hauglustaine, D., Boone, C. D., and Bernath, P. F.: ACE-FTS observation of a young biomass burning plume: first reported measurements of C_2H_4, C_3H_6O, H_2CO and PAN by infrared occultation from space, Atmos. Chem. Phys. Discuss., 7, 7907–7932, 2007, http://www.atmos-chem-phys-discuss.net/7/7907/2007/.

Connors, V. S., Gormsen, B. B., Nolf, S., and Reichle, H. G., et al.: Spaceborne observations of the global distribution of carbon monoxide in the middle troposphere during April and October 1994, J. Geophys. Res., 104, 21 455–21 470, 1999.

Deeter, M. N., Emmons, L. K., Edwards, D. P., Gille, J. C., and Drummond, J. R.: Vertical resolution and information content of CO profiles retrieved by MOPITT, Geophys. Res. Lett., 31, L15112, doi:10.1029/2004GL020235, 2004.

Dethof, A., O'Neill, A., Slingo, J. M., and H. G. J. Smit, H. G. J.: A mechanism for moistening the lower stratosphere involving the Asian summer monsoon, Q. J. R. Meteorol. Soc., 125, 1079–1106, 1999.

Dufour, G., Boone, C. D., Rinsland, C. P., and Bernath, P. F.: First space-borne measurements of methanol inside aged southern tropical to mid-latitude biomass burning plumes using the ACE-FTS instrument, Atmos. Chem. Phys., 6, 3463–3470, 2006, http://www.atmos-chem-phys.net/6/3463/2006/.

Edwards, D. P., Emmons, L. K., Gille, J. C., et al.: Satellite-observed pollution from Southern Hemisphere biomass burning, J. Geophys. Res., 111, D14312, doi:10.1029/2005JD006655, 2006.

Folkins, I., and Martin, R.: The vertical structure of tropical convection and its impact on the budgets of water vapor and ozone. J. Atmos. Sci., 62, 1560–1573, 2005.

Fu, R., Hu, Y., Wright, J. S., Jiang, J. H., Dickinson, R. E., Chen, M., Filipiak, M., Read, W. G., Waters, J. W., Wu, D. L.:Short circuit of water vapor and polluted air to the global stratosphere by convective transport over the Tibetan Plateau, Proc. Nat. Acad. Sci., 103, 5664–5669, 2006.

Gettelman, A., Salby, M. L., and Sassi, F.: Distribution and influence of convection in the tropical tropopause region, J. Geophys. Res., 107(D10), 4080, doi:10.1029/2001JD001048, 2002.

Jacob, D. J., Crawford, J. H., Kleb, M. M., Connors, V. S., Bendura, R. J., Raper, J. L., Sachse,

G. W., Gille, J. C., Emmons, L., and Heald, C. L.: The Transport and Chemical Evolution over the Pacific (TRACE-P) aircraft mission: design, execution, and first results, J. Geophys. Res., 108 (D20), 1–19, 2003.

Jin J. J., Semeniuk, K., Jonsson, A. I., et al.: Co-located ACE-FTS and Odin/SMR stratospheric-mesospheric CO 2004 measurements and comparison with a GCM, Geophys. Res. Lett., 32, L15S03, doi:10.1029/2005GL022433, 2005.

Krishnamurti, T. N. and Bhalme, H. N.: Oscillations of a monsoon system. Part I. Observational aspects, J. Atmos. Sci., 33, 1937–1954, 1976.

Li, Q., Jacob, D. J., Bey, I., Yantosca, R. M., Zhao, Y., Kondo, Y., and Notholt, J.: Atmospheric hydrogen cyanide (HCN): Biomass burning source, ocean sink?, Geophys. Res. Lett., 27, 357–360, 2000.

Li, Q., Jiang, J. H., Wu, D. L., Read, W. G., Livesey, N. J., Waters, J. W., Zhang, Y., Wang, B., Filipiak, M. J., Davis, C. P., Turquety, S., Wu, S., Park, R. J., Yantosca, R. M., and Jacob, D. J.: Trapping of Asian pollution by the Tibetan anticyclone: A global CTM simulation compared with EOS MLS observations, Geophys. Res. Lett., 32, L14826, doi:10.1029/2005GL022762, 2005.

Liu, C. and Zipser, E. J.: Global distribution of convection penetrating the tropical tropopause, J. Geophys. Res., 110, D23104, doi:10.1029/2005JD006063, 2005.

Logan, J. A., Prather, M. J., Wofsy, S. C., and McElroy, M. B.: Tropospheric chemistry – A global perspective, J. Geophys. Res., 86, 7210–7254, 1981.

Park, M., Randel, W. J., Gettelman, A., Massie, S. T., and Jiang, J. H.: Transport above the Asian summer monsoon anticyclone inferred from Aura Microwave Limb Sounder tracers, J. Geophys. Res., 112, D16309, doi:10.1029/2006JD008294, 2007.

Randel, W. J., and Park, M.: Deep convective influence on the Asian summer monsoon anticyclone and associated tracer variability observed with Atmospheric Infrared Sounder (AIRS), J. Geophys. Res., 111, D12314, doi:10.1029/2005JD006490, 2006.

Rinsland, C. P., Dufour, G., Boone, C. D., Bernath, P. F., and Chiou, L.: Atmospheric Chemistry Experiment (ACE) measurements of elevated Southern Hemisphere upper tropospheric CO, C_2H_6, HCN, and C_2H_2 mixing ratios from biomass burning emissions and long-range transport, Geophys. Res. Lett., 32, L20803, doi:10.1029/2005GL024214, 2005.

Singh, H. B., Salas, L., Herlth, D., Kolyer, R., Czech, E., Viezee, W., Li, Q., Jacob, D. J., Blake, D., Sachse, G., Harward, C. N., Fuelberg, H., Kiley, C. M., Zhao, Y., and Kondo, Y.: In situ measurements of HCN and CH_3CN over the Pacific Ocean: Sources, sinks, and budgets, J.

Geophys. Res., 108(D20), 8795, doi:10.1029/2002JD003006, 2003.
Smyth, S., Bradshaw, J., Sandholm, S., et al.: Comparison of free tropospheric western Pacific air mass classification schemes for the PEM-West A experiment, J. Geophys. Res., 101, 1743–1762, 1996.
Smyth, S., Sandholm, S., Shumaker, B., et al.: Characterization of the chemical signatures of air masses observed during the PEM experiments over the western Pacific, J. Geophys. Res., 104, 16 243–16 254, 1999.
Talbot, R. W., Dibb, J. E., Scheuer, E. M., Blake, D. R., Blake, N. J., Gregory, G. L., Sachse, G. W., Bradshaw, J. D., Sandholm, S. T., and Singh, H. B.: Influence of biomass combustion emissions on the distribution of acidic trace gases over the southern Pacific basin during Austral springtime, J. Geophys. Res., 104, 5623–5634, 1999.
Walker, K. A., Randall, C. E., Trepte, C. R., Boone, C. D., and Bernath, P. F.: Initial validation comparisons for the Atmospheric Chemistry Experiment (ACE-FTS), Geophys. Res. Lett., 32, L16S04, doi:10.1029/2005GL022388, 2005.
Watts, S. F.: The mass budgets of carbonyl sulfide, dimethyl sulfide, carbon disulfide and hydrogen sulfide, Atmos. Environ., 34, 761–779, 2000.
Waters, J. W., Froidevaux, L., Harwood, R. S., et al.: The Earth Observing System Microwave Limb Sounder (EOS MLS) on the Aura satellite, IEEE Trans. Geosci. Remote Sens., 44(5), 1075–1092, 2006.
Xiao Y., Jacob, D. J., and Turquety, S.: Atmospheric acetylene and its relationship with CO as an indicator of air mass age, J. Geophys. Res., 112, D12305, doi:10.1029/2006JD008268, 2007.
Yoshida, Y., Wang, Y., Zeng, T., and Yantosca, R.: A three-dimensional global model study of atmospheric methylchloride budget and distributions, J. Geophys. Res., 109, D24309, doi:10.1029/2004JD004951, 2004.
Zhao, Y., Strong, K., Kondo, Y., Koike, M., Matsumi, Y., Irie, H., Rinsland, C. P., Jones, N. B., Suzuki, K., Nakajima, H., Nakane, H., and Murata, I.: Spectroscopic measurements of tropospheric CO, C_2H_6, C_2H_2, and HCN in northern Japan, J. Geophys. Res., 107(D18), 4343, doi:10.1029/2001JD000748, 2002.

Table 1. Photochemical lifetimes.

Species	Lifetime
CO	2–3 months [a]
HCN	5 months [c,d,e]
C_2H_6	1–2 months [b,d]
C_2H_2	0.5–1 months [a,b]
CH_3Cl	1 year [b,f,i]
OCS	4.3 years [g,h]

[a] Xiao et al., 2007
[b] Logan et al., 1981
[c] Li et al., 2000
[d] Zhao et al., 2002
[e] Singh et al., 2003
[f] Blake et al., 1996
[g] Blake et al., 2004
[h] Chin and Davis, 1996
[i] Yoshida et al., 2004

ACPD
7, 13839–13860, 2007

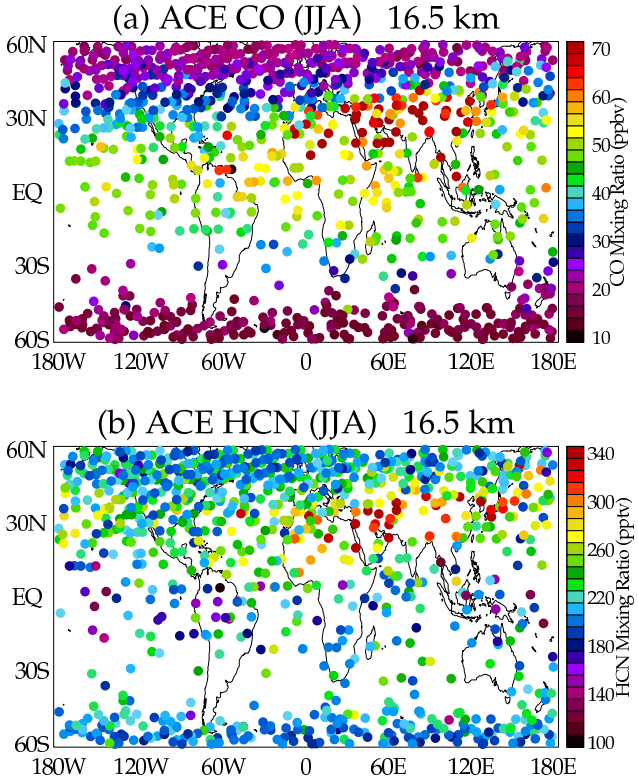

Fig. 1. Global map of **(a)** CO and **(b)** HCN mixing ratios at 16.5 km for June–August (2004–2006). Approximate data range is 10–70 parts per billion by volume (ppbv) for CO and 100–340 parts per trillion by volume (pptv) for HCN.

ACPD
7, 13839–13860, 2007

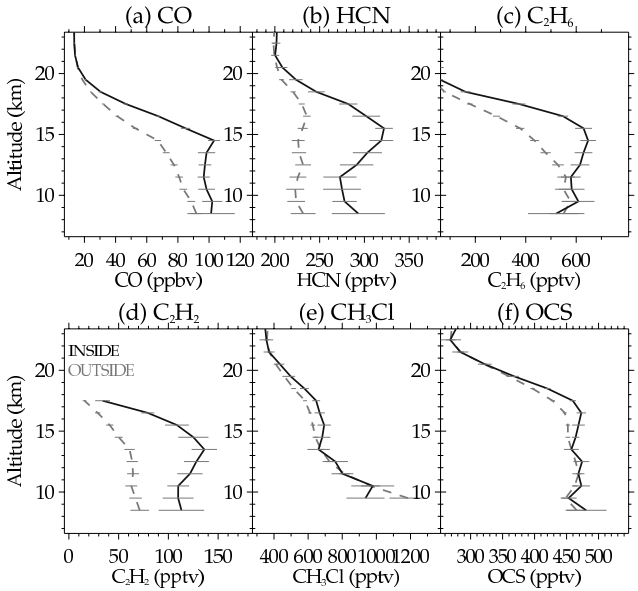

Fig. 2. Average profile of tropospheric tracers (a-CO, b-HCN, c-C_2H_6, d-C_2H_2, e-CH_3Cl, and f-OCS) inside (solid) and outside (dashed) of the monsoon anticyclone, respectively. Two-sigma standard error from the mean is denoted as solid line.

ACPD
7, 13839–13860, 2007

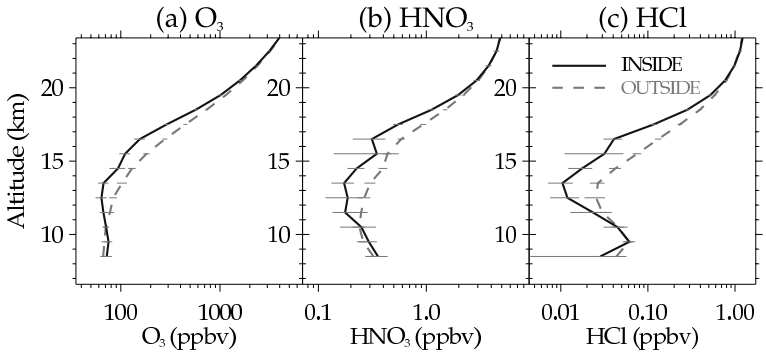

Fig. 3. Same as Fig. 2 but for stratospheric tracers (a-O_3, b-HNO_3 and c-HCl). Note the stratospheric tracers have log-scale x-axis.

ACPD
7, 13839–13860, 2007

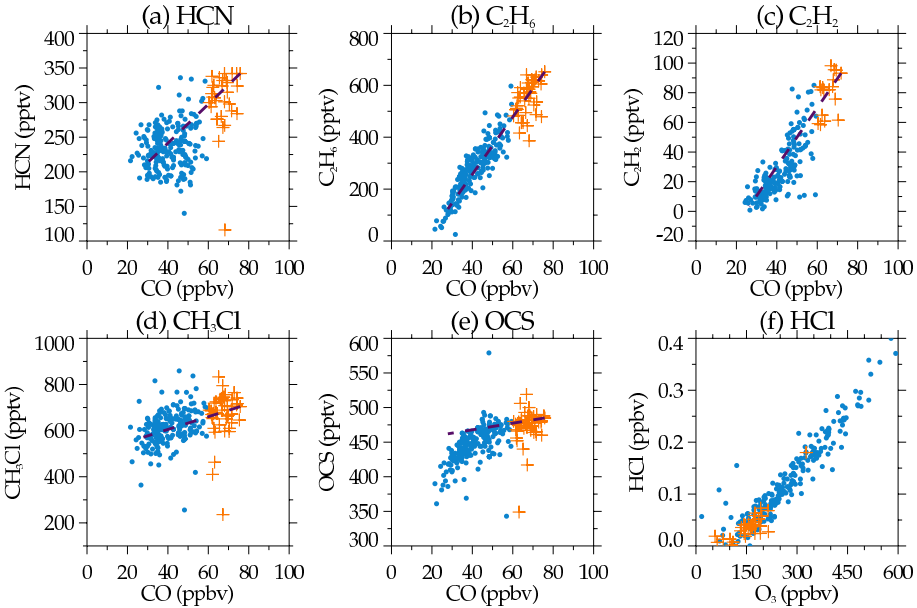

Fig. 4. Scatter plots of CO (ppbv) versus **(a)** HCN (pptv), **(b)** C_2H_6 (pptv), **(c)** C_2H_2 (pptv), **(d)** CH_3Cl (pptv) and **(e)** OCS (pptv), and **(f)** O_3 (ppbv) versus HCl (ppbv) at 16.5 km. Pluses indicate measurements inside and dots indicate outside of the monsoon anticyclone, respectively. The dashed line in each panel is derived from the photochemical lifetimes of each species (see text for detail).

ACPD
7, 13839–13860, 2007

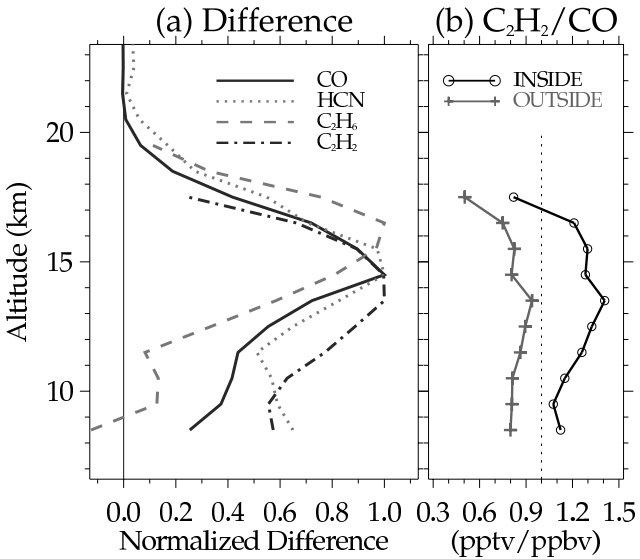

Fig. 5. **(a)** Normalized difference between average profiles inside and outside the anticyclone for the tropospheric tracers, i.e., CO (solid), HCN (dotted), C_2H_6 (dashed), and C_2H_2 (dash dot). **(b)** Ratio of C_2H_2/CO inside (open circle) and outside (plus) the anticyclone, respectively.

ACPD
7, 13839–13860, 2007

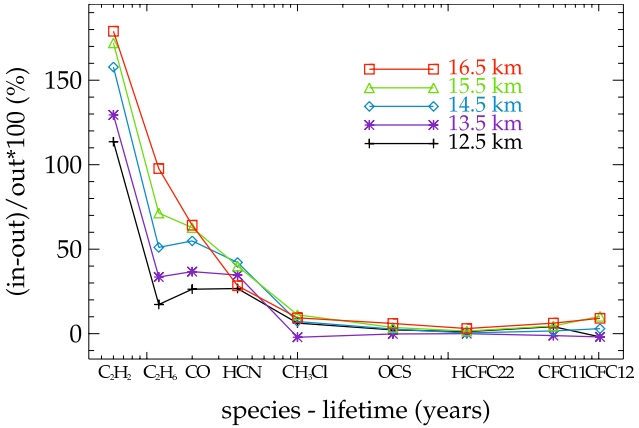

Fig. 6. Level of enhancement (%) of the tropospheric tracers over 12.5–16.5 km. The log-scale x-axis represents the chemical lifetime of the tracers in years (CH_3Cl–1 year).

ACPD
7, 13839–13860, 2007

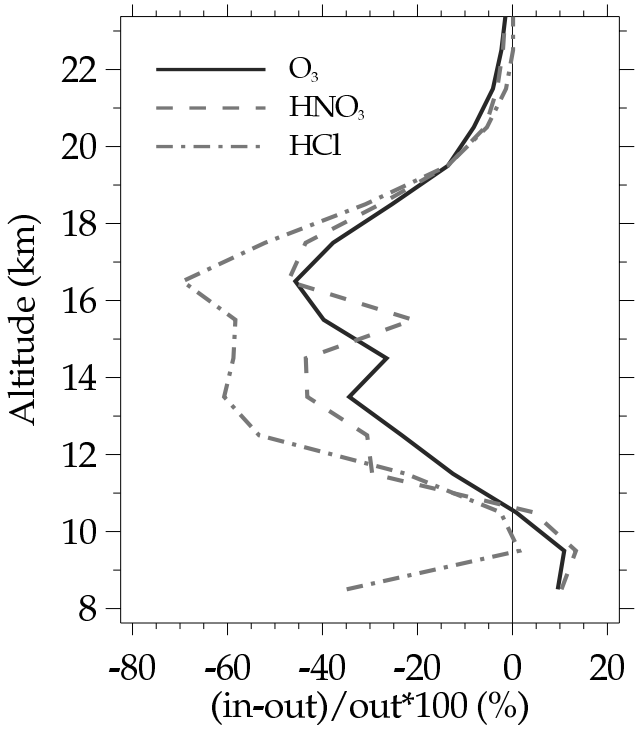

Fig. 7. Level of enhancement (%) of the stratospheric tracers, O_3 (solid), HNO_3 (dashed), and HCl (dash dot).

ACPD
7, 13839–13860, 2007